1521-009X/45/4/390–398$25.00
DRUG METABOLISM AND DISPOSITION

http://dx.doi.org/10.1124/dmd.116.074450
Drug Metab Dispos 45:390–398, April 2017

Application of Physiologically Based Pharmacokinetic Modeling to the Understanding of Bosutinib Pharmacokinetics: Prediction of Drug–Drug and Drug–Disease Interactions[S]

Chiho Ono, Poe-Hirr Hsyu, Richat Abbas, Cho-Ming Loi, and Shinji Yamazaki

Clinical Pharmacology, Pfizer Japan Inc., Tokyo, Japan (C.O.); Clinical Pharmacology, Pfizer Inc., San Diego, California (P.-H.H.); Clinical Pharmacology, Pfizer Essential Health, Collegeville, Pennsylvania (R.A.); and Pharmacokinetics, Dynamics, and Metabolism, Pfizer Worldwide Research and Development, San Diego, California (C.-M.L., S.Y.)

Received November 29, 2016; accepted February 3, 2017

ABSTRACT

Bosutinib is an orally available Src/Abl tyrosine kinase inhibitor indicated for the treatment of patients with Philadelphia chromosome–positive chronic myelogenous leukemia. Bosutinib is predominantly metabolized by CYP3A4 as the primary clearance mechanism. The main objectives of this study were to 1) develop physiologically based pharmacokinetic (PBPK) models of bosutinib; 2) verify and refine the PBPK models based on clinical study results of bosutinib single-dose drug–drug interaction (DDI) with ketoconazole and rifampin, as well as single-dose drug–disease interaction (DDZI) in patients with renal and hepatic impairment; 3) apply the PBPK models to predict DDI outcomes in patients with weak and moderate CYP3A inhibitors; and 4) apply the PBPK models to predict DDZI outcomes in renally and hepatically impaired patients after multiple-dose administration. Results showed that the PBPK models adequately predicted bosutinib oral exposures in patients after single- and multiple-dose administrations. The PBPK models also reasonably predicted changes in bosutinib exposures in the single-dose DDI and DDZI results, suggesting that the PBPK models were sufficiently developed and verified based on the currently available data. Finally, the PBPK models predicted 2- to 4-fold increases in bosutinib exposures by moderate CYP3A inhibitors, as well as comparable increases in bosutinib exposures in renally and hepatically impaired patients between single- and multiple-dose administrations. Given the challenges in conducting numerous DDI and DDZI studies of anticancer drugs in patients, we believe that the PBPK models verified in our study would be valuable to reasonably predict bosutinib exposures under various scenarios that have not been tested clinically.

Introduction

Understanding how certain extrinsic and intrinsic factors influence systemic exposures of new molecular entities (NMEs) in patients is crucial for drug development and regulatory decision making (Zhao et al., 2011; Huang and Rowland, 2012; Zhang et al., 2012; Chang et al., 2013). Changes in drug exposures by these factors can potentially lead to differences in therapeutic and/or adverse responses, such that it is critical to appropriately optimize dosing regimens of NMEs, particularly anticancer agents with narrow therapeutic windows. One important extrinsic factor is coadministered drugs, which may change NME exposures through inhibition or induction of drug-metabolizing enzymes and/or transporters [i.e., drug–drug interaction (DDI)]. The U.S. Food and Drug Administration (FDA), the European Medicines Agency, and the Japanese Pharmaceuticals and Medical Devices Agency issued individual DDI guidances that underscore the predictive use of integrated mechanistic approaches such as a physiologically based pharmacokinetic (PBPK) model as a tool for quantitative DDI assessment (http://www.fda.gov/downloads/Drugs/GuidanceComplianceRegulatoryInformation/Guidances/ucm292362.pdf, http://www.ema.europa.eu/docs/en_GB/document_library/Scientific_guideline/2012/07/WC500129606.pdf, and http://www.nihs.go.jp/mss/T140710-jimu.pdf, respectively). Since most drugs are mainly eliminated from the body through metabolism and excretion in the liver and kidneys, impaired organ function in the liver and kidneys [i.e., drug–disease interaction (DDZI)] is one important intrinsic factor that can modulate drug exposures. The FDA and the European Medicines Agency issued guidances to investigate the pharmacokinetics of NMEs in renally and hepatically impaired patients (RIPs and HIPs, respectively), providing recommendations on study design and data analysis as well as impact on dosing and labeling (http://www.fda.gov/downloads/drugs/guidancecomplianceregulatoryinformation/guidances/ucm072123.pdf, http://www.fda.gov/downloads/Drugs/Guidances/UCM204959.pdf, http://www.ema.europa.eu/docs/en_GB/document_library/Scientific_guideline/2009/09/WC500003122.pdf, and http://www.ema.europa.eu/docs/en_GB/document_library/Scientific_guideline/2014/02/WC500162133.pdf).

Bosutinib (Bosulif; Pfizer, New York, NY) is an orally available Src/Abl tyrosine kinase inhibitor and was recently approved globally for the treatment of adult patients with chronic, accelerated, or blast-phase

This research was supported by Pfizer Inc.
dx.doi.org/10.1124/dmd.116.074450.
[S]This article has supplemental material available at dmd.aspetjournals.org.

ABBREVIATIONS: AUC, area under the plasma concentration-time curve; AUCR, area under the plasma concentration-time curve ratio; CL, plasma clearance; CL_{int}, intrinsic clearance; CP, cancer patient; DDI, drug–drug interaction; DDZI, drug–disease interaction; FDA, U.S. Food and Drug Administration; HIP, hepatically impaired patient; HV, healthy volunteer; NME, new molecular entity; P450, cytochrome P450; PBPK, physiologically based pharmacokinetics; RIP, renally impaired patient; t_{max}, time to reach C_{max}; USPI, U.S. prescribing information; V_{ss}, steady-state volume of distribution.

Philadelphia chromosome–positive chronic myelogenous leukemia with resistance or intolerance to prior therapy (http://www.accessdata.fda.gov/drugsatfda_docs/label/2016/203341s006lbl.pdf; Pfizer, 2016). Bosutinib is predominantly metabolized by CYP3A4 as the primary clearance mechanism in humans with minimal urinary excretion (<2% of the administered dose as the parent drug) (Syed et al., 2014; CDER, 2012). As one of the potential risk assessments for extrinsic factors, single-dose bosutinib DDI studies with a strong CYP3A inhibitor (ketoconazole) and a strong CYP3A inducer (rifampin) were conducted in healthy volunteers (HVs) (Abbas et al., 2012a, 2015). In these studies, ketoconazole increased bosutinib's maximum plasma concentration (C_{max}) by approximately 3-fold and its area under the plasma concentration-time curve (AUC) by approximately 5-fold, whereas rifampin decreased bosutinib C_{max} and AUC by 86% and 94%, respectively. Accordingly, the U.S. prescribing information (USPI) advises to avoid concurrent use of bosutinib with strong or moderate CYP3A inhibitors and inducers (Pfizer, 2016). In addition, the FDA issued a postmarketing requirement to evaluate effects of moderate CYP3A4 inhibitors (e.g., erythromycin) on bosutinib exposures to recommend appropriate dosing regimens when bosutinib is used concomitantly with moderate CYP3A inhibitors (http://www.accessdata.fda.gov/drugsatfda_docs/nda/2012/203341Orig1s000ClinPharmR.pdf). To assess the potential risks of intrinsic factors, the effects of impaired organ function on single-dose bosutinib pharmacokinetics were investigated in RIPs and HIPs (http://www.accessdata.fda.gov/drugsatfda_docs/nda/2012/203341Orig1s000ClinPharmR.pdf). Increases in bosutinib exposures were approximately 1.5-fold in moderate and severe RIPs, whereas they were approximately 2-fold in HIPs with Child–Pugh scores A, B, and C (Pugh et al., 1973). Accordingly, the USPI recommends adjusting the dosage for RIPs and HIPs (Pfizer, 2016). However, changes in bosutinib exposures have not yet been evaluated in multiple-dose DDZI studies, since it is challenging to recruit patients in sufficient numbers for multiple-dose administration studies of anticancer drugs. There are also ethical concerns, with possible supratherapeutic exposures in such clinical studies.

PBPK modeling is a powerful predictive approach to quantitatively extrapolate in vitro and in silico drug-dependent parameters to in vivo pharmacokinetics based on drug-independent physiologic parameters; thus, its application in drug development has increased in recent years, as illustrated by several excellent reviews (Lavé et al., 2007; Nestorov, 2007; Rowland et al., 2011; Jones and Rowland-Yeo, 2013; Jones et al., 2015). Consequently, growing emphasis is being placed on PBPK modeling to quantitatively predict the magnitude of in vivo DDIs and DDZIs of NMEs (Rowland et al., 2011; Huang and Rowland, 2012; Prueksaritanont et al., 2013; Wagner et al., 2015). Accordingly, it would be highly beneficial to develop a PBPK model of bosutinib to quantitatively predict effects of extrinsic and intrinsic factors on bosutinib exposures in patients. The main objectives of our study were to 1) develop PBPK models of bosutinib, 2) verify and refine the PBPK models based on currently available clinical results, 3) apply the PBPK models to predict DDI outcome in cancer patients (CPs) with weak and moderate CYP3A inhibitors, and 4) apply the PBPK models to predict DDZI outcomes in RIPs and HIPs after multiple-dose administration.

Materials and Methods

Clinical Pharmacokinetic Data

Detailed information about bosutinib clinical studies, such as single-dose pharmacokinetics in CPs, DDI studies with ketoconazole and rifampin in HVs, and DDZI studies with RIPs and HIPs, was previously reported (Cortes et al., 2011; Abbas et al., 2012b, 2013, 2015; Daud et al., 2012). Additional information about bosutinib pharmacokinetics is also available on the FDA website (http://www.accessdata.fda.gov/drugsatfda_docs/nda/2012/203341Orig1s000ClinPharmR.pdf). Briefly, bosutinib pharmacokinetics were determined in HVs (n = 12) and CPs (n = 3) after a single oral administration of a clinically recommended dose at 500 mg (Cortes et al., 2011; Hsyu et al., 2017). Bosutinib steady-state pharmacokinetics were determined in CPs (n = 3) after multiple-dose oral administration at 500 mg once daily (Cortes et al., 2011). A single-dose DDI study of bosutinib with ketoconazole in HVs (n = 56) was conducted in a two-way crossover design with a 14-day washout period (Abbas et al., 2012a). Each subject received a single oral dose of 500 mg bosutinib (day 2) either alone or with 5-day repeated oral doses of 400 mg ketoconazole once daily (days 1–5). A single-dose DDI study with rifampin was conducted in HVs (n = 24) (Abbas et al., 2015). Each subject received a single oral dose of 500 mg bosutinib (days 1 and 14) with 10-day repeated oral doses of 600 mg rifampin once daily (days 8–17). In a single-dose DDZI study with RIPs, 200 mg bosutinib was orally administered to moderate and severe RIPs (n = 8/group) defined as creatinine clearance of 30–50 and <30 ml/min, respectively, along with HVs (n = 8) as a control group (creatinine clearance >80 ml/min) (Abbas and Hsyu, 2016). In a single-dose DDZI study with HIPs, 200 mg bosutinib was orally administered to HIPs with Child–Pugh scores A, B, and C (n = 6 each), along with HVs (n = 9) as a control group (Abbas et al., 2013).

Bosutinib Input Parameters in PBPK Models

A commercially available dynamic PBPK model, Simcyp population-based simulator version 13.1 (Simcyp Limited, Sheffield, UK), was used for all simulations (Jamei et al., 2009). The physicochemical and pharmacokinetic parameters of bosutinib used for the PBPK models are summarized in Table 1. A fraction of the dose absorbed (F_a) at the 500-mg dose was estimated at approximately 0.7, since the recovery of bosutinib (as the parent drug) in feces was 30% of the administered oral dose in a single oral-dose human mass-balance study with [^{14}C]bosutinib at 500 mg, and fecal recovery of bosutinib was unlikely confounded by biliary excretion of the unchanged drug and/or reversible metabolites based on the metabolic profiling results in the mass-balance study (http://www.accessdata.fda.gov/drugsatfda_docs/nda/2012/203341Orig1s000ClinPharmR.pdf). Accordingly, bosutinib F_a was set at 0.7 at the dose of 500 mg. In DDZI studies with RIPs and HIPs at the 200-mg dose, observed AUC estimates (993 and 714 ng·h/ml, respectively) in the control groups were 10%–40% lower than the dose-normalized AUC value (1104 ng·h/ml) calculated from the AUC estimate at 500 mg assuming a dose proportionality between 200 and 500 mg. Therefore, predicted F_a values in the DDZI studies with RIPs and HIPs were adjusted to 0.6 and 0.5, respectively, by the differences in dose-normalized AUC values. Bosutinib renal clearance was estimated to be 0.9 l/h based on urinary excretion (approximately 2% of the administered dose as the parent drug) in the human mass-balance study CDER, 2012). An input parameter of hepatic microsomal intrinsic clearance (CL_{int}) in bosutinib PBPK models was back-calculated from the clinically observed oral plasma clearance (CL/F_{oral}) using a retrograde model implemented in Simcyp. The back-calculated CL_{int} values were 300 μl/min per mg microsomal proteins from the CL/F_{oral} estimate of 200 l/h (189–207 l/h) at the oral doses of 500 mg in CPs (Cortes et al., 2011; Daud et al., 2012). The fraction of bosutinib metabolized by CYP3A4 ($f_{m,CYP3A4}$) was estimated as near unity based on the in vitro cytochrome P450 (P450) phenotyping and the human mass-balance study CDER, 2012). Therefore, the back-calculated CL_{int} value was assigned to CYP3A4-mediated CL_{int} in the PBPK models. Bosutinib steady-state volume of distribution (V_{ss}) was predicted to be 15 l/kg, based on a single-species scaling with an exponent of unity from mice, rats, and dogs (12, 12–19, and 14 l/kg, respectively) after correction for species differences in unbound fractions in plasma ($f_{u,plasma}$), which were 0.059, 0.061, and 0.041, respectively (Hosea et al., 2009; CDER, 2012). Therefore, the predicted V_{ss} of 7.5 l/kg by the tissue composition–based model implemented in Simcyp (as the mathematical model 2) was adjusted to 15 l/kg using a K_p scalar of 2 (Rodgers et al., 2005).

To predict bosutinib plasma concentration-time profiles, the full-PBPK models implemented in Simcyp were used with the first-order absorption models (Simcyp, 2013). For DDZI prediction in HIPs, Foti (2014) previously reported that a full-PBPK model in Simcyp considerably overpredicted changes in drug oral exposures, which was likely due to physiologic parameters related to shunting of blood flow away from the liver. Therefore, we performed the bosutinib DDZI

TABLE 1

Physicochemical and pharmacokinetic parameters of bosutinib in PBPK models

Parameter	Value	Source
Molecular weight	531	Calculated
logP	3.1	Measured
pK_a (monobase)	7.9	Measured
$f_{u,plasma}$	0.063	Measured
B/P	1.2	Measured
F_a	0.5–0.7	Estimated from the mass-balance study results
k_a (h^{-1})	0.13	Estimated from the clinical study results
Lag time (h)	1	Estimated from the clinical study results
$P_{eff,man}$ (10^{-4} cm/s)	1.8	Calculated from physiochemical property
Q_{gut} (l/h)	8.7	Calculated by Simcyp
$f_{u,gut}$	1	Assumed (Simcyp default)
V_{ss} (l/kg)	15	Predicted from nonclinical results
$CL_{int,CYP3A4}$ (μl/min per mg protein)	300	Back-calculated from the observed CL/F_{oral}
CL_{renal} (l/h)	0.9	Estimated from the mass-balance study results
k_{in}/k_{out} (h^{-1})[a]	0.039/0.021	Estimated from the two-compartment PK analysis

[a]Distribution rate constants for a single adjustment compartment in minimal-PBPK models used for simulation in HIPs.

prediction in HIPs by minimal-PBPK models with a single adjustment compartment (Simcyp, 2013). Bosutinib input parameters of a single adjustment compartment were as follows: V_{ss} of 9.7 l/kg, with k_{in} of 0.039 h^{-1} and k_{out} of 0.021 h^{-1} based on pharmacokinetic analyses with two-compartment models.

PBPK Modeling and Simulation

Our modeling and simulation approaches were basically categorized into three main tiers: 1) model development, 2) model verification/refinement, and 3) model application. For model development, bosutinib PBPK models were developed based on in vitro and in vivo data, and bosutinib exposures were then predicted in HVs after a single oral administration. The predicted results were also compared between virtual populations of HVs and CPs because the single- and multiple-dose pharmacokinetic data were obtained from phase I studies with CPs, whereas the single-dose DDI studies with ketoconazole and rifampin were conducted in HVs. For model verification and refinement, PBPK model-predicted bosutinib exposures were compared with clinically observed results in the single-dose DDI and DDZI studies to evaluate the predictive model performance. For model application, bosutinib single-dose DDI outcomes with weak and moderate CYP3A inhibitors and multiple-dose DDZI outcomes in RIPs and HIPs were predicted by the PBPK models. An outline of these simulation trials is summarized in Table 2. For bosutinib DDI prediction with weak and moderate CYP3A inhibitors, erythromycin (250 mg four times a day), fluconazole (200 mg once daily), fluvoxamine (50 mg once daily), and verapamil (120 mg three times a day) were used for PBPK modeling. The compound files of ketoconazole (sim-ketoconazole 400 mg daily), rifampin (sim-rifampicin), erythromycin (sim-erythromycin), fluconazole (sv-fluconazole), fluvoxamine (sv-fluvoxamine), and verapamil (sim-verapamil) from the Simcyp compound library were used for the DDI predictions. Default DDI parameters on CYP3A4 were as follows: ketoconazole [competitive $K_i = 0.015$ μM ($f_{u,mic} = 0.97$)], rifampin [induction $E_{max} = 16$, $EC_{50} = 0.32$ μM, and competitive $K_i = 10.5$ μM ($f_{u,mic} = 1$)], erythromycin [competitive $K_i = 82$ μM ($f_{u,mic} = 0.909$), mechanism-based inhibition $k_{inact} = 2.25$ h^{-1}, and $K_I = 23.2$ μM ($f_{u,mic} = 1$)], fluconazole [competitive $K_i = 10.7$ μM ($f_{u,mic} = 1$)], fluvoxamine [$K_i = 17.89$ μM ($f_{u,mic} = 0.441$)], and verapamil [mechanism-based inhibition $k_{inact} = 2.0$ h^{-1} and $K_I = 2.21$ μM ($f_{u,mic} = 1$)].

Simulation of all clinical trials was performed in Simcyp with a virtual population in a fed state in 10 trials of 10 subjects (total of 100 subjects), as the USPI recommends that bosutinib be taken with food. The output sampling interval in a Simcyp simulation tool box was set at 0.2 hours in all simulations. Virtual populations used from the Simcyp default population library were as follows: HVs; moderate and severe RIPs with glomerular filtration rates of 30–60 ml/min and $<$ 30 ml/min, respectively; and mild, moderate, and severe HIPs with Child–Pugh scores A, B, and C, respectively. Key features of the Simcyp virtual population of RIPs and HIPs are as follows (Johnson et al., 2010; Rowland Yeo et al., 2011; Simcyp, 2013): features for RIPs include 1) reduced kidney weight and blood flow, 2) reduced hepatic P450 expression (e.g., CYP2B6, CYP2C9, CYP2D6, and CYP3A4), and 3) reduced serum albumin and hematocrit levels, whereas features for HIPs include 1) reduced liver size, 2) reduced hepatic P450 expression (e.g., CYP1A2, CYP2C19, CYP2D6, and CYP3A4), 3) reduced serum albumin and α-1 acid glycoprotein levels, and 4) altered blood flows, such as reduced hepatic portal blood flow or portal hypertension with consequential blood shunting to bypass the liver with increased blood flow through the hepatic artery and mesentery.

For a virtual population of CPs, the demographic characteristics in a population file of HVs were changed based on those of CPs previously reported (e.g., age, body weights, plasma protein level, and hematocrit) (Cheeti et al., 2013).

TABLE 2

Simulation outline of bosutinib DDI and DDZI studies for model verification and application

Study	Population	Bosutinib Dose	Treatment Day	Precipitant	Dose	Treatment Day	Analysis
		mg			*mg*		
DDI	HVs	500	2	Ketoconazole	400 QD	1–5	Predicted versus observed
			7	Rifampin	600 QD	1–10	Predicted versus observed
			5	Fluvoxamine	50 QD	1–8	Predicted
			5	Fluconazole	200 QD	1–8	Predicted
			5	Erythromycin	250 QID	1–8	Predicted
			5	Verapamil	120 TID	1–8	Predicted
DDZI	RIPs	200	1	–	–	–	Predicted versus observed
			1–28	–	–	–	Predicted
	HIPs	200	1	–	–	–	Predicted versus observed
			1–28	–	–	–	Predicted

Dashes indicate not applicable. QD, once daily; QID, four times a day; TID, three times a day.

TABLE 3

Clinically observed and PBPK model-predicted pharmacokinetic parameters of bosutinib in subjects after single and multiple oral administrations of 500 mg bosutinib once daily

Data are expressed as geometric means with percent coefficients of variation in parentheses (n = 3 in the observed results in CPs, n = 12 in the observed results in HVs, and n = 100 in the predicted results; 10 individuals × 10 groups).

Population	Analysis	Single Dose		Multiple Doses	
		C_{max}	AUC	C_{max}	AUC
		ng/ml	*ng·h/ml*	*ng/ml*	*ng·h/ml*
CPs	Observed	97 (35)	2030 (23)	200 (72)	3640 (51)
	Predicted	74 (55)	1789 (58)	135 (63)	2403 (69)
	P/O	0.8	0.9	0.7	0.7
HVs	Observed	95 (39)	2193 (38)	–	–
	Predicted	80 (47)	2445 (65)	–	–
	P/O	0.8	1.1	–	–

Dashes indicate not applicable.

Data Analysis

Pharmacokinetic parameters such as C_{max}, time to reach C_{max} (t_{max}) and AUC over the dosing interval were obtained from Simcyp outputs. The ratio of predicted or observed C_{max} (C_{max}R) and AUC (AUCR) in treatment groups relative to control groups were calculated in the DDI and DDZI studies. In addition, $f_{m,CYP3A4}$ values at each simulation time point were individually calculated from simulated CL_{int} values in each pathway divided by total CL_{int} values in the Simcyp output files. Fractions of the dose that escapes hepatic and intestinal first-pass elimination (i.e., F_h and F_g, respectively) at each simulation timepoint were individually calculated by the well stirred and Q_{gut} models, respectively (Yang et al., 2007). Thereafter, median $f_{m,CYP3A4}$, F_h, and F_g values were calculated during drug treatment. All of these calculations in Simcyp output files were performed with Microsoft Excel 2007 (Microsoft, Redmond, WA).

To estimate the predictive performance of the PBPK models, the ratios of predicted-to-observed pharmacokinetic parameters (P/O) were calculated by the following equation:

$$\mathrm{P/O} = \frac{\text{Predicted parameter}}{\text{Observed parameter}}$$

P/O ratios of 0.7–1.4 were used as the predefined criteria to assess the predictive performance of the PBPK models.

Results

Model Development

Prediction of Bosutinib Pharmacokinetics in CPs and HVs. After a single oral dose of 500 mg bosutinib, clinically observed bosutinib pharmacokinetics were comparable between CPs and HVs (Table 3). The PBPK model-predicted plasma concentration-time profiles of bosutinib adequately matched the observed results in both CPs and HVs after a single oral administration of 500 mg bosutinib (Fig. 1). Predicted C_{max} and AUC values were comparable to the observed results, with P/O ratios of 0.8–1.1 (Table 3). In PBPK modeling, predicted hepatic and intestinal CL_{int}, $f_{u,plasma}$, blood-to-plasma ratios (B/P), and unbound fractions in the blood ($f_{u,blood}$) were also comparable between virtual populations of CPs and HVs (Supplemental Table 1). After multiple oral doses of 500 mg bosutinib once daily, the model-predicted plasma concentration-time profiles of bosutinib sufficiently matched the observed results, with a P/O ratio of 0.7 for C_{max} and AUC (Table 3). Overall, these results suggested that bosutinib PBPK models were reasonably developed based on the in vitro and in vivo data.

Model Verification and Refinement

Prediction of Bosutinib DDI with Ketoconazole. A single oral dose of 500 mg bosutinib was administered to HVs either as bosutinib alone (control group) or bosutinib on day 2 with coadministration of 400 mg ketoconazole once daily from days 1 to 5 (treatment group). The clinically observed bosutinib C_{max} and AUC values were 107 ng/ml and 1980 ng·h/ml in the control group and 315 ng/ml and 10,500 ng·h/ml in the treatment group, respectively, resulting in a C_{max}R of 2.9 and an AUCR of 5.3 (Table 4). Plasma concentrations of bosutinib in both groups were adequately predicted by the PBPK models (Fig. 2A). The predicted C_{max} and AUC were comparable to the observed results, with P/O ratios of 0.8–1.3; this resulted in a reasonable prediction for C_{max}R and AUCR, with P/O ratios of 1.1–1.3 (Table 4). In PBPK modeling, bosutinib $f_{m,CYP3A4}$ in a virtual population decreased from 0.98 to 0.77 by coadministration of ketoconazole, whereas F_h and F_g increased from 0.63 to 0.92 and 0.56 to 0.89, respectively. Overall, the PBPK models sufficiently predicted the effect of ketoconazole on bosutinib exposures in HVs.

Prediction of Bosutinib DDI with Rifampin. A single oral dose of 500 mg bosutinib was administered to HVs either as bosutinib alone (control group) on day 1 or bosutinib on day 14 with coadministration of 600 mg rifampin once daily from days 8 to 17 (treatment group). The clinically observed bosutinib C_{max} and AUC values were 109 ng/ml and 2350 ng·h/ml in the control group and 15 ng/ml and 149 ng·h/ml in the treatment group, respectively, resulting in a C_{max}R of 0.14 and an AUCR of 0.06 (Table 4). Plasma concentrations of bosutinib in both groups were reasonably predicted by the PBPK models (Fig. 2B). The predicted AUC values were comparable to the observed results, with P/O ratios of 1.0–1.1, whereas C_{max} values were slightly underpredicted, with the P/O ratios of 0.8 and 0.6 in the control and treatment groups, respectively (Table 4). The C_{max}R and the AUCR were reasonably predicted, with P/O ratios of 0.8–0.9. The predicted bosutinib $f_{m,CYP3A4}$ in a virtual population increased slightly from 0.98 to 0.99 during rifampin treatment, whereas the predicted F_h and F_g decreased from 0.63 to 0.21 and 0.56 to 0.15, respectively. Overall, the PBPK models adequately predicted the effect of rifampin on bosutinib exposures in HVs.

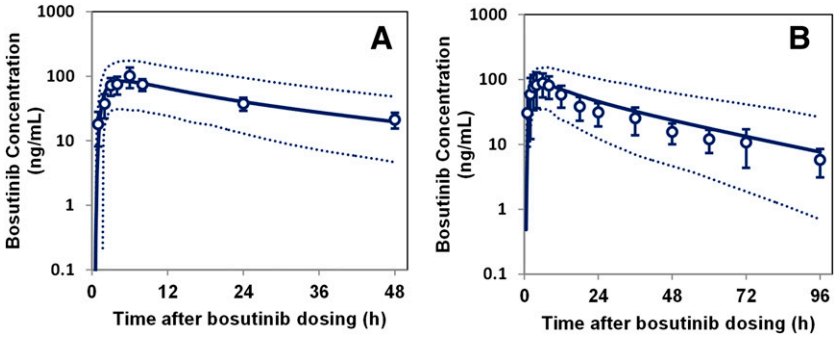

Fig. 1. PBPK model-predicted and observed plasma concentrations of bosutinib in CPs (A) and HVs (B) after a single oral administration of 500 mg bosutinib. The x-axis represents the time after dosing in hours, and the y-axis represents the predicted (lines) and observed (open circles) plasma concentrations in nanograms per milliliter on a logarithmic scale. The predicted and observed plasma concentrations are expressed as the mean (solid lines) with 5th and 95th percentiles (dashed lines) and the mean ± S.D., respectively.

TABLE 4

Clinically observed and PBPK model-predicted pharmacokinetic parameters of bosutinib in healthy subjects after a single oral administration of 500 mg bosutinib with and without repeated coadministration of 400 mg ketoconazole and 600 mg rifampin once daily

Data are expressed as geometric means with percent coefficients of variation in parentheses.

Precipitant	Analysis	Control Group		Treatment Group		Ratio[a]	
		C_{max}	AUC	C_{max}	AUC	C_{max}R	AUCR
		ng/ml	*ng·h/ml*	*ng/ml*	*ng·h/ml*		
Ketoconazole	Observed	107 (35)	1980 (35)	315 (24)	10,500 (27)	2.9	5.3
	Predicted	83 (42)	2407 (49)	314 (31)	13,698 (37)	3.8	5.7
	P/O	0.8	1.2	1.0	1.3	1.3	1.1
Rifampin	Observed	109 (26)	2350 (28)	15 (42)	149 (34)	0.14	0.06
	Predicted	83 (42)	2575 (51)	8.9 (87)	145 (91)	0.11	0.06
	P/O	0.8	1.1	0.6	1.0	0.8	0.9

[a]Ratios of C_{max} and AUC in the treatment group (bosutinib with ketoconazole or rifampin) to the control group (bosutinib alone).

Prediction of Bosutinib DDZI in RIPs. A single oral dose of 200 mg bosutinib was administered to moderate and severe RIPs, along with HVs as the control. The clinically observed C_{max} and AUC values were 33 ng/ml and 993 ng·h/ml in HVs, 42 ng/ml and 1404 ng·h/ml in moderate RIPs, and 44 ng/ml and 1575 ng·h/ml in severe RIPs, respectively. Thus, the C_{max}R and the AUCR were 1.3 and 1.4 in moderate RIPs and 1.3 and 1.6 in severe RIPs, respectively (Table 5). The PBPK models reasonably predicted plasma concentrations of bosutinib in all of the groups (Fig. 3). The predicted C_{max} and AUC were comparable to the observed results, with P/O ratios of 0.9–1.1; as a result, the C_{max}R and the AUCR were adequately predicted, with P/O ratios of 1.1–1.2 (Table 5). The model-predicted hepatic CYP3A4 abundances in moderate and severe RIPs (3.6 and 3.0 $\times$ 10^6 pmol/liver, respectively) were 50%– 60% lower than those in HVs (7.1 $\times$ 10^6 pmol/liver) (Supplemental Table 2). Consequently, the decreases in model-predicted individual CYP3A4 abundances in the liver were associated with the increases in model-predicted individual AUC values in the virtual populations (Supplemental Fig. 1). On the other hand, the predicted individual $f_{u,blood}$ did not correlate well with the predicted individual AUC values. The difference in predicted $f_{u,blood}$ values between HVs (0.053) and moderate to severe RIPs (0.059–0.069) was minimal (i.e., 1.1- to 1.3-fold) (Supplemental Table 2). Overall, the PBPK models sufficiently predicted the increases in bosutinib exposures in moderate and severe RIPs, which could be largely caused by the decrease in hepatic CYP3A4 abundances.

Prediction of Bosutinib DDZI in HIPs. A single oral dose of 200 mg bosutinib was administered to HIPs with Child–Pugh scores A, B, and C, along with HVs as the control. The clinically observed C_{max} and AUC values in HVs and HIPs with Child–Pugh A, B, and C were 32 ng/ml and 714 ng·h/ml, 78 ng/ml and 1720 ng·h/ml, 64 ng/ml and 1350 ng·h/ml, and 49 ng/ml and 1270 ng·h/ml, respectively. As a result, the observed AUCRs in HIPs with Child–Pugh A, B, and C were 2.4, 1.9, and 1.8, respectively, whereas the C_{max}Rs were 2.4, 2.0, and 1.5, respectively (Table 6). Thus, bosutinib exposures in HIPs were roughly 2-fold higher than those in HVs, with an apparent trend of slight decreases in the exposures with increasing severity of hepatic impairment. The PBPK models did not predict bosutinib exposures well in HIPs, as the P/O ratios for C_{max}R and AUCR varied from 0.6 to 2.0 (Table 6).

To improve the predictive model performance, bosutinib F_a values in HIPs with Child–Pugh A, B, and C were back-calculated at 0.68, 0.35, and 0.23, respectively, based on the P/O ratios of AUC with an F_a of 0.5 in HVs. That is, the decrease in F_a in HIPs was assumed in PBPK modeling, as discussed later. Using the back-calculated F_a values, the PBPK models adequately predicted bosutinib exposures in HIPs with Child–Pugh A, B, and C (Fig. 4). The predicted AUC and AUCR were comparable to the observed results, with P/O ratios of 0.9–1.0, whereas the C_{max} and C_{max}R were slightly underpredicted, with P/O ratios of 0.5–0.8 (Table 6). In PBPK modeling, the predicted CYP3A4 abundances in virtual populations of HIPs with Child–Pugh A, B, and C decreased with increasing disease severity, with 4.0, 2.1, and 1.2 $\times$ 10^6 pmol/liver, in the liver and 0.042, 0.032, and 0.022 $\times$ 10^6 pmol/intestines in the intestines, respectively (Supplemental Table 2). These CYP3A4 abundances in the liver and intestines were 40%–80% and 20%–60% lower than those in HVs (7.1 $\times$ 10^6 pmol/liver and 0.056 $\times$ 10^6 pmol/intestines), respectively. The decreases in model-predicted individual CYP3A4 abundances in the virtual populations were associated with the increases in predicted individual AUC values (Supplemental Fig. 2). On the other hand, the predicted individual $f_{u,blood}$ did not correlate well with the predicted AUC values. The difference in the predicted $f_{u,blood}$ between HVs (0.053) and HIPs (0.062–0.10) was minimal (i.e., 1.2- to 1.9-fold) (Supplemental Table 2). Overall, the PBPK models sufficiently predicted the increases in bosutinib exposures in HIPs with Child–Pugh A, B, and C, assuming the decrease in F_a.

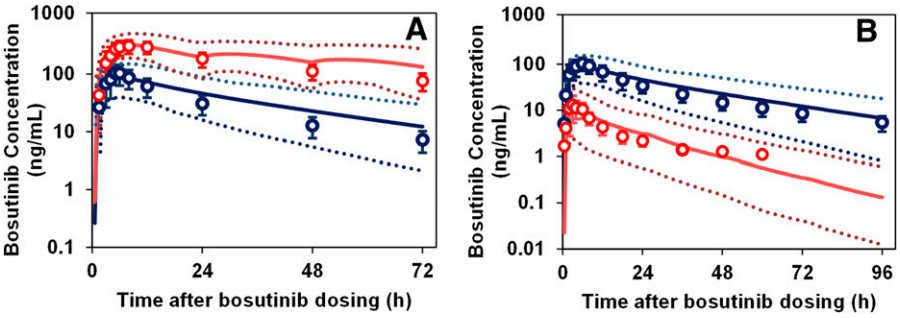

Fig. 2. PBPK model-predicted and observed plasma concentrations of bosutinib in HVs after a single oral administration of 500 mg bosutinib with (red) and without (blue) coadministration of 400 mg ketoconazole once daily (A) and 600 mg rifampin once daily (B). The *x*-axis represents the time after dosing in hours, and the *y*-axis represents the predicted (lines) and observed (open circles) plasma concentrations in nanograms per milliliter on a logarithmic scale. The predicted and observed plasma concentrations are expressed as the mean (solid lines) with 5th and 95th percentiles (dashed lines) and the mean ± S.D., respectively.

TABLE 5

Clinically observed and PBPK model-predicted pharmacokinetic parameters of bosutinib in subjects with renal impairment after a single oral administration of 200 mg bosutinib

Data are expressed as geometric means with percent coefficients of variation in parentheses or as median t_{max} values with ranges in parentheses.

Population	Analysis	PK Parameter			Ratio[a]	
		C_{max}	t_{max}	AUC	C_{max}R	AUCR
		ng/ml	*h*	*ng·h/ml*		
HVs	Observed	33 (46)	5.0 (2.0–6.0)	993 (37)	–	–
	Predicted	30 (43)	5.2 (3.0–7.8)	944 (53)	–	–
	P/O	0.9	–	1.0	–	–
Moderate RIPs	Observed	42 (23)	5.0 (3.0–12)	1404 (44)	1.3	1.4
	Predicted	41 (49)	6.0 (3.8–10)	1566 (55)	1.4	1.7
	P/O	1.0	–	1.1	1.1	1.2
Severe RIPs	Observed	44 (30)	6.0 (3.0–12)	1575 (34)	1.3	1.6
	Predicted	42 (48)	6.0 (4.0–11)	1611 (54)	1.4	1.7
	P/O	1.0	–	1.0	1.1	1.1

Dashes indicate not applicable.
[a]Ratios of C_{max} and AUC in RIPs to HVs.

Model Application

Prediction of Bosutinib DDIs with Weak and Moderate CYP3A Inhibitors. Bosutinib DDIs with weak and moderate CYP3A inhibitors were predicted by the PBPK models. In these DDI predictions, a single oral dose of 500 mg bosutinib was administered to a virtual population of HVs on day 5 with and without 9-day repeated coadministration of fluvoxamine (50 mg once daily), fluconazole (200 mg once daily), erythromycin (250 mg four times a day), or verapamil (120 mg three times a day). The PBPK model-predicted plasma concentration-time profiles are graphically presented in Supplemental Fig. 3. The predicted bosutinib C_{max} and AUC with CYP3A inhibitors were 84 ng/ml and 2603 ng·h/ml with fluvoxamine, 190 ng/ml and 8689 ng·h/ml with fluconazole, 210 ng/ml and 10,197 ng·h/ml with erythromycin, and 181 ng/ml and 7466 ng·h/ml with verapamil, respectively (Table 7). Correspondingly, the predicted C_{max}R and AUCR by the moderate inhibitors were 2.3 and 3.4 with fluconazole, 2.5 and 4.0 with erythromycin, and 2.4 and 3.1 with verapamil, respectively, whereas those with the weak inhibitor, fluvoxamine, were 1.0. Thus, the increases in bosutinib exposures with moderate CYP3A inhibitors were predicted to be 2- to 4-fold. In addition, the model-predicted bosutinib $f_{m,CYP3A4}$ decreased from 0.98 to 0.94–0.95 by the moderate CYP3A inhibitors, whereas the model-predicted F_h and F_g increased from 0.63 to 0.74–0.85 and 0.56 to 0.78–0.93, respectively.

Prediction of Multiple-Dose DDZIs in RIPs and HIPs. To obtain PBPK model-predicted bosutinib steady-state exposures in RIPs and HIPs, multiple oral doses of 200 mg bosutinib once daily were administered to virtual populations of moderate and severe RIPs, along with HVs (Supplemental Fig. 4), and to virtual populations of HIPs with Child–Pugh A, B, and C, along with HVs (Supplemental Fig. 5). In RIPs, the predicted C_{max}R and AUCR on day 28 were 1.7 and 1.8 in moderate RIPs and 1.7 and 1.9 in severe RIPs, , respectively (Table 8). Thus, the predicted increases in bosutinib steady-state exposures in moderate and severe RIPs were comparable to those after a single-dose administration. In HIPs, the predicted C_{max}R and AUCR on day 28 were 2.3 and 2.5 for Child–Pugh A, 1.9 and 2.2 for Child–Pugh B, and 1.8 and 2.2 for Child–Pugh C, respectively (Table 8). Therefore, the predicted increases in bosutinib exposures in HIPs were also comparable between single- and multiple-dose administrations.

Discussion

We have developed and verified PBPK models to understand the effects of extrinsic and intrinsic factors on bosutinib pharmacokinetics. This practice has become common in drug development and regulatory decision making (Zhao et al., 2012; Huang et al., 2013; Sinha et al., 2014; Jones et al., 2015). Bosutinib PBPK models appear to be successful in providing predictive DDI and DDZI outcomes. However, some issues have been identified and warrant further discussion.

In the single-dose mass-balance study with HVs (500 mg), fecal recovery of bosutinib as the parent drug was approximately 30% of the administered dose CDER, 2012. Fecal recovery was considered to be a fraction of the unabsorbed dose ($1 - F_a$), because it was unlikely confounded by biliary excretion of the unchanged drug and/or reversible metabolites based on the metabolic profiling results (CDER, 2012). Thus, bosutinib F_a at the 500-mg dose was set at 0.7 in the PBPK models assuming that F_a was comparable between HVs and CPs. Baker et al. (2004) previously reported that CYP3A activity did not change with age, sex, and body size measurements in 134 CPs. Consistently, PBPK model-predicted exposures of the CYP3A probe substrate, midazolam, were comparable between HVs and CPs (Cheeti et al., 2013). In our study, model-predicted bosutinib exposures were also comparable between these populations (Table 3). In the DDZI studies (200 mg), bosutinib F_a was adjusted to 0.5–0.6 to sufficiently recover the observed exposures in the control groups. The F_a adjustment suggested that bosutinib F_a slightly decreased from the doses of 500 to 200 mg, although the differences might be within interindividual/study variability. Clinically observed increases in bosutinib exposures were supra-proportional at doses of 50–200 mg, whereas they were roughly dose proportional at the higher doses of 200–600 mg (Hsyu et al., 2014; CDER, 2012). Since bosutinib is a substrate of P-glycoprotein, nonlinear-to-linear pharmacokinetics at the lower-to-higher doses would be considered mainly due to a saturation of intestinal P-glycoprotein–mediated efflux, resulting in increases in F_a at doses up to around 200 mg. Thus, the slight increase in

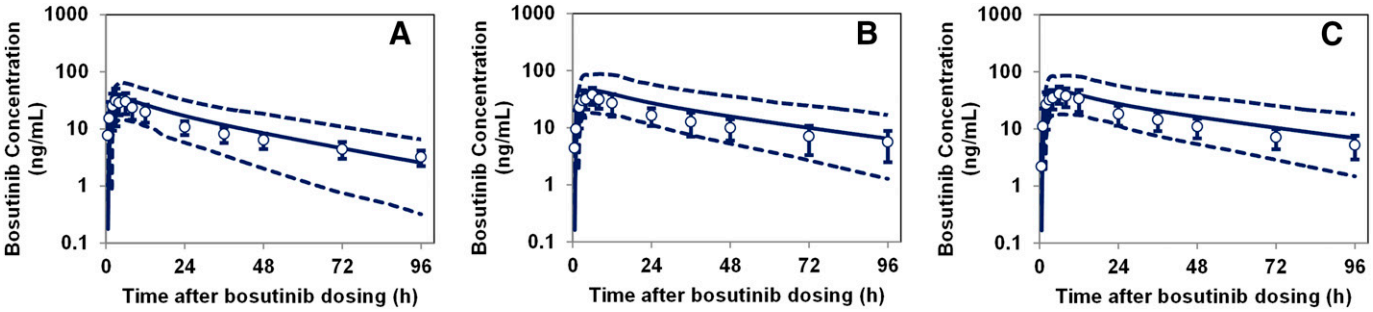

Fig. 3. PBPK model-predicted and observed plasma concentrations of bosutinib in HVs (A) and patients with moderate (B) and severe (C) renal impairment after a single oral administration of 200 mg bosutinib. The *x*-axis represents the time after dosing in hours, and the *y*-axis represents the predicted (lines) and observed (open circles) plasma concentrations in nanograms per milliliter on a logarithmic scale. The predicted and observed plasma concentrations are expressed as the mean (solid lines) with 5th and 95th percentiles (dashed lines) and the mean ± S.D., respectively.

TABLE 6

Clinically observed and PBPK model-predicted pharmacokinetic parameters of bosutinib in subjects with hepatic impairment after a single oral administration of 200 mg bosutinib

Data are expressed as geometric means with percent coefficients of variation in parentheses or as median t_{max} values with ranges in parentheses.

Population	Analysis	PK Parameter				Ratio[b]	
		F_a[a]	C_{max}	t_{max}	AUC	C_{max}R	AUCR
			ng/ml	*h*	*ng·h/ml*		
HVs	Observed	–	32 (31)	4.0 (1.0–8.0)	714 (43)	–	–
	Predicted	0.50	29 (43)	3.4 (2.6–4.7)	752 (53)	–	–
	P/O	–	0.9	–	1.1	–	–
HIPs							
Child–Pugh A	Observed	–	78 (52)	2.5 (0.5–4.0)	1720 (26)	2.4	2.4
	Predicted	0.50	39 (44)	2.0 (1.6–2.7)	1265 (59)	1.4	1.7
	P/O	–	0.5	–	0.7	0.6	0.7
	Predicted	0.68	53 (42)	2.0 (1.6–2.7)	1710 (58)	1.8	2.3
	P/O	–	0.7	–	1.0	0.8	1.0
Child–Pugh B	Observed	–	64 (35)	2.0 (1.0–4.0)	1350 (40)	2.0	1.9
	Predicted	0.50	48 (38)	2.1 (1.6–2.9)	1942 (50)	1.7	2.6
	P/O	–	0.8	–	1.4	0.8	1.4
	Predicted	0.35	34 (38)	2.1 (1.6–2.9)	1359 (50)	1.2	1.8
	P/O	–	0.5	–	1.0	0.6	1.0
Child–Pugh C	Observed	–	49 (70)	1.5 (1.0–3.0)	1270 (47)	1.5	1.8
	Predicted	0.50	59 (34)	2.0 (1.6–2.7)	2734 (43)	2.1	3.6
	P/O	–	1.2	–	2.2	1.4	2.0
	Predicted	0.23	27 (34)	2.0 (1.6–2.7)	1257 (43)	0.9	1.7
	P/O	–	0.6	–	1.0	0.6	0.9

Dashes indicate not applicable.
[a]Predicted F_a was first fixed at 0.5 and then calculated from the simulation results with F_a of 0.5.
[b]Ratios of C_{max} and AUC in HIPs to HVs.

F_a from the doses of 200 to 500 mg could be consistent with the clinical findings.

In the DDI study with ketoconazole, the observed bosutinib AUCR was consistent with that expected from coadministration of a strong CYP3A4 inhibitor (i.e., >5-fold) (Zhao et al., 2009; http://www.fda.gov/downloads/Drugs/GuidanceComplianceRegulatoryInformation/Guidances/ucm292362.pdf). According to a postmarketing requirement, a clinical DDI study with a moderate CYP3A inhibitor, aprepitant (125 mg), was recently conducted in HVs (Hsyu et al., 2017). The observed bosutinib AUCR with aprepitant was approximately 2-fold, which appeared to be consistent with the PBPK model-predicted AUCR with the moderate CYP3A inhibitors in our study. In PBPK modeling, the predicted bosutinib F_h and F_g were approximately 0.6, which increased to near unity by coadministration of ketoconazole, suggesting that the increase in bosutinib exposures could be caused by CYP3A inhibition in both the liver and intestines. In the DDI prediction with moderate CYP3A inhibitors fluconazole, erythromycin, and verapamil, the predicted bosutinib F_h and F_g increased to 0.74–0.85 and 0.78–0.93, respectively. Thus, the moderate inhibitors could also inhibit CYP3A4-mediated metabolism of bosutinib in both the liver and intestines. In the DDI study with rifampin, the predicted F_h and F_g decreased to 0.2, suggesting that the decrease in bosutinib exposures by rifampin could be

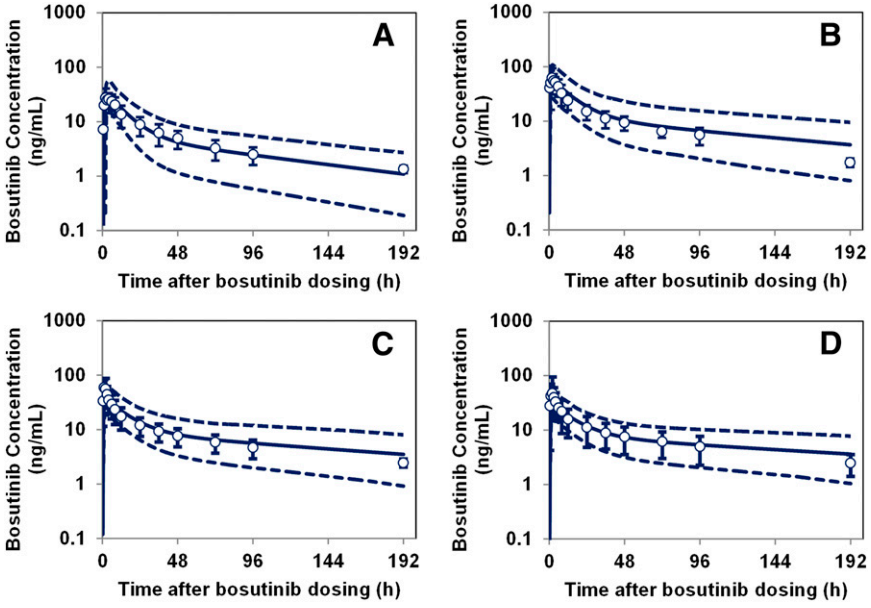

Fig. 4. PBPK model-predicted and observed plasma concentrations of bosutinib in HVs (A) and hepatically impaired patients with Child–Pugh scores A (B), B (C), and C (D) after a single oral administration of 200 mg bosutinib. The *x*-axis represents the time after dosing in hours, and the *y*-axis represents the predicted (lines) and observed (open circles) plasma concentrations in nanograms per milliliter on a logarithmic scale. The predicted and observed plasma concentrations are expressed as the mean (solid lines) with 5th and 95th percentiles (dashed lines) and the mean ± SD, respectively.

TABLE 7

PBPK model-predicted pharmacokinetic parameters of bosutinib in healthy subjects after a single oral administration of bosutinib with repeated coadministration of weak and moderate CYP3A inhibitors

Data are expressed as geometric means with percent coefficients of variation in parentheses.

Precipitant	PK Parameter		Ratio[a]	
	C_{max}	AUC	C_{max}R	AUCR
	ng/ml	*ng·h/ml*		
Fluvoxamine	84 (42)	2603 (51)	1.0	1.0
Fluconazole	190 (34)	8689 (40)	2.3	3.4
Erythromycin	210 (36)	10,197 (50)	2.5	4.0
Verapamil	181 (41)	7466 (63)	2.4	3.1

[a]Ratios of C_{max} and AUC in the treatment group (bosutinib with CYP3A inhibitor) to the control group (bosutinib alone).

caused by CYP3A4 induction in both the liver and intestines. Thus, PBPK modeling could provide a quantitative framework with mechanistic insights to further understand in vivo DDIs.

The most obvious changes caused by chronic kidney disease are decreases in renal clearance. In addition, the disease is also associated with other changes such as reduced plasma protein binding and drug-metabolizing enzyme activity, particularly CYP3A (Sun et al., 2006; Dreisbach and Lertora, 2008; Zhang et al., 2009). Thus, the pharmacokinetics of most drugs, including those that are primarily metabolized by CYP3A, should be evaluated in RIPs to provide appropriate dosing recommendation (http://www.fda.gov/downloads/Drugs/Guidances/UCM204959.pdf and http://www.ema.europa.eu/docs/en_GB/document_library/Scientific_guideline/2014/02/WC500162133.pdf). The observed increases in bosutinib exposures in moderate and severe RIPs (i.e., approximately 1.5-fold) were comparable to those for the CYP3A probe substrate, midazolam (Vinik et al., 1983). The model-predicted hepatic CYP3A4 abundances in RIPs were inversely associated with the predicted bosutinib exposures (Supplemental Fig. 1). On the other hand, the potential changes in plasma protein binding can be another important factor for bosutinib pharmacokinetics. However, the clinically observed bosutinib ex vivo $f_{u,plasma}$ values were comparable between HVs and RIPs (e.g., 0.040–0.081). The model-predicted $f_{u,plasma}$ values in RIPs were only 1.1- to 1.3-fold higher than those in HVs, and the predicted $f_{u,blood}$ did not correlate well with the predicted individual AUC (Supplemental Fig. 1). Thus, the changes in plasma protein levels in RIPs did not appear to significantly affect bosutinib pharmacokinetics.

It is well known that cirrhosis not only reduces the expression of drug-metabolizing enzymes and transporters but also changes hepatic architecture, leading to the development of blood shunting to bypass the liver with increased blood flow through the hepatic artery and mesentery (Elbekai et al., 2004; Verbeeck, 2008). There appear to be considerable challenges to accurately incorporating these physiologic changes into PBPK models (particularly, portal-systemic blood shunting). As a result, PBPK models, specifically full-PBPK models in Simcyp, tend to overpredict drug exposures in HIPs (Foti, 2014). Accordingly, we performed the DDZI prediction in HIPs with minimal-PBPK models, which had fewer physiologic parameters, especially those related to blood shunting (Simcyp, 2013; Foti, 2014).

In the clinical DDZI study with HIPs, the observed apparent, slight but consistent, decrease in bosutinib exposures with increasing severity of hepatic impairment was not expected from the results of other CYP3A substrates (Verbeeck, 2008; Johnson et al., 2010). Therefore, the PBPK models did not predict bosutinib exposures well in HIPs (when F_a was fixed at 0.5) (Table 6). In PBPK modeling, the predicted CYP3A4 abundances in the liver and intestines of virtual populations decreased with increasing disease severity by 1.8- to 6.2-fold and 1.3- to 2.5-fold, respectively, relative to HVs (Supplemental Table 2). The model-predicted individual CYP3A4 abundances were inversely associated with bosutinib exposures (Supplemental Fig. 2). These findings suggested that some other factors in HIPs could (in part) offset the increases in bosutinib exposures caused by the decrease in CYP3A4-mediated clearance. For plasma protein binding, the clinically observed bosutinib ex vivo $f_{u,plasma}$ values were comparable between HVs and HIPs (http://www.accessdata.fda.gov/drugsatfda_docs/nda/2012/203341Orig1s000ClinPharmR.pdf). The PBPK model-predicted individual $f_{u,blood}$ did not correlate well with the predicted AUC values, although the model-predicted $f_{u,blood}$ values in HIPs were 1.2- to 1.9-fold higher than those in HVs (Supplemental Fig. 2; Supplemental Table 2). Thus, the changes in $f_{u,blood}$ did not appear to offset the increase in bosutinib exposures due to the decrease in CYP3A abundances.

In addition to reducing drug-metabolizing enzymes and plasma proteins, cirrhosis also decreases gastrointestinal absorption due to congestion and decreased blood flow in the intestinal mucosa (Elbekai et al., 2004; Verbeeck, 2008). Consistently, the observed bosutinib t_{max} decreased with the increasing disease severity from 4.0 in HVs to 2.5, 2.0, and 1.5 hours in HIPs with Child–Pugh A, B, and C, respectively, in parallel with the decrease in observed C_{max}Rs of 2.4, 2.0, and 1.5, respectively CDER, 2012. Therefore, the absorption of bosutinib could possibly be altered in patients with varying degrees of hepatic impairment. In contrast, the observed apparent terminal half-life was approximately 2-fold longer in HIPs (86–113 hours) than HVs

TABLE 8

PBPK model-predicted pharmacokinetic parameters of bosutinib in patients with renal and hepatic impairment after multiple oral administration of 200 mg bosutinib

Data are expressed as geometric means with percent coefficients of variation in parentheses or as median t_{max} values with ranges in parentheses (n = 10 per group × 10 groups).

Study	Population	PK Parameter				Ratio[b]	
		F_a[a]	C_{max}	t_{max}	AUC	C_{max}R	AUCR
			ng/ml	*h*	*ng·h/ml*		
RIPs	HVs	0.60	57 (51)	4.4 (3.0–6.2)	1029 (57)	–	–
	Moderate RIPs	0.60	95 (57)	4.9 (3.6–7.0)	1861 (62)	1.7	1.8
	Severe RIPs	0.60	98 (57)	5.0 (3.8–6.8)	1941 (62)	1.7	1.9
HIPs	HVs	0.50	52 (49)	3.4 (2.6–4.6)	854 (56)	–	–
	Child–Pugh A	0.68	120 (60)	2.8 (2.0–4.0)	2117 (70)	2.3	2.5
	Child–Pugh B	0.35	97 (57)	2.8 (2.0–4.0)	1870 (64)	1.9	2.2
	Child–Pugh C	0.23	94 (51)	2.6 (2.0–4.0)	1899 (56)	1.8	2.2

Dashes indicate not applicable.
[a]Predicted F_a was fixed at the values used for the single-dose simulation.
[b]Ratios of C_{max} and AUC in RIPs or HIPs to HVs.

(55 hours), which appeared to be consistent with the decrease in CYP3A-mediated clearance of bosutinib due to enzyme abundances. Accordingly, we hypothesized that the decrease in bosutinib F_a in HIPs could (in part) offset the increase in exposures caused by the decrease in CYP3A4-mediated clearance. Accordingly, the F_a values were back-calculated based on the P/O ratios of AUC values with an F_a of 0.5 in HVs. As a result, the model-predicted AUCR (1.7–2.3) was comparable to the observed results (1.8–2.4), whereas the C_{max}R was still slightly underpredicted by approximately 2-fold (Table 6). Thus, we would need more mechanistic absorption models to predict bosutinib C_{max} in HIPs. We, however, believe that our PBPK models could be sufficient to predict multiple-dose DDZI outcomes.

In conclusion, our study demonstrates that bosutinib PBPK models have adequately been developed, verified, and refined based on currently available data such as single-dose DDI and DDZI studies; therefore, the models can be applied to predict bosutinib exposures in single-dose DDI studies with other P450 inhibitors and multiple-dose DDZI studies. The DDI prediction suggested 2- to 4-fold increases in bosutinib exposures by moderate CYP3A inhibitors. The DDZI prediction suggested that the fold increases in bosutinib exposures in RIPs and HIPs would be comparable between single- and multiple-dose administrations. Given the challenges in conducting numerous DDI and DDZI studies of anticancer drugs in CPs, it would be highly beneficial to develop PBPK models to quantitatively predict their exposures under various scenarios that have not yet been tested clinically. We believe that bosutinib dose adjustments in CPs could be reasonably recommended by the PBPK models developed and verified in this study.

Acknowledgments

The authors thank Bhasker Shetty (Pharmacokinetics, Dynamics, and Metabolism, Pfizer, San Diego, CA) for valuable discussion about bosutinib pharmacokinetics.

Authorship Contributions

Participated in research design: Ono, Yamazaki.

Performed data analysis: Ono, Yamazaki.

Wrote or contributed to the writing of the manuscript: Ono, Hsyu, Abbas, Loi, Yamazaki.

References

Abbas R, Boni J, and Sonnichsen D (2015) Effect of rifampin on the pharmacokinetics of bosutinib, a dual Src/Abl tyrosine kinase inhibitor, when administered concomitantly to healthy subjects. *Drug Metab Pers Ther* **30**:57–63.

Abbas R, Chalon S, Leister C, El Gaaloul M, and Sonnichsen D (2013) Evaluation of the pharmacokinetics and safety of bosutinib in patients with chronic hepatic impairment and matched healthy subjects. *Cancer Chemother Pharmacol* **71**:123–132.

Abbas R and Hsyu PH (2016) Clinical pharmacokinetics and pharmacodynamics of bosutinib. *Clin Pharmacokinet* **55**:1191–1204.

Abbas R, Hug BA, Leister C, and Sonnichsen D (2012a) A randomized, crossover, placebo- and moxifloxacin-controlled study to evaluate the effects of bosutinib (SKI-606), a dual Src/Abl tyrosine kinase inhibitor, on cardiac repolarization in healthy adult subjects. *Int J Cancer* **131**: E304–E311.

Abbas R, Leister C, El Gaaloul M, Chalon S, and Sonnichsen D (2012b) Ascending single-dose study of the safety profile, tolerability, and pharmacokinetics of bosutinib coadministered with ketoconazole to healthy adult subjects. *Clin Ther* **34**:2011.e1–2019.e1.

Baker SD, van Schaik RH, Rivory LP, Ten Tije AJ, Dinh K, Graveland WJ, Schenk PW, Charles KA, Clarke SJ, Carducci MA, et al. (2004) Factors affecting cytochrome P-450 3A activity in cancer patients. *Clin Cancer Res* **10**:8341–8350.

Chang Y, Burckart GJ, Lesko LJ, and Dowling TC (2013) Evaluation of hepatic impairment dosing recommendations in FDA-approved product labels. *J Clin Pharmacol* **53**:962–966.

Cheeti S, Budha NR, Rajan S, Dresser MJ, and Jin JY (2013) A physiologically based pharmacokinetic (PBPK) approach to evaluate pharmacokinetics in patients with cancer. *Biopharm Drug Dispos* **34**:141–154.

Cortes JE, Kantarjian HM, Brümmendorf TH, Kim DW, Turkina AG, Shen ZX, Pasquini R, Khoury HJ, Arkin S, Volkert A, et al. (2011) Safety and efficacy of bosutinib (SKI-606) in chronic phase Philadelphia chromosome-positive chronic myeloid leukemia patients with resistance or intolerance to imatinib. *Blood* **118**:4567–4576.

Daud AI, Krishnamurthi SS, Saleh MN, Gitlitz BJ, Borad MJ, Gold PJ, Chiorean EG, Springett GM, Abbas R, Agarwal S, et al. (2012) Phase I study of bosutinib, a Src/Abl tyrosine kinase inhibitor, administered to patients with advanced solid tumors. *Clin Cancer Res* **18**:1092–1100.

Dreisbach AW and Lertora JJ (2008) The effect of chronic renal failure on drug metabolism and transport. *Expert Opin Drug Metab Toxicol* **4**:1065–1074.

Elbekai RH, Korashy HM, and El-Kadi AO (2004) The effect of liver cirrhosis on the regulation and expression of drug metabolizing enzymes. *Curr Drug Metab* **5**:157–167.

Foti RS (2014) Strategies and retrospective data analysis in hepatic impairment studies, in *Proceedings of the 19th North American Regional ISSX Meeting*; 2014 Oct 19–23; San Francisco, CA. International Society for the Study of Xenobiotics, Washington, DC.

Hosea NA, Collard WT, Cole S, Maurer TS, Fang RX, Jones H, Kakar SM, Nakai Y, Smith BJ, Webster R, et al. (2009) Prediction of human pharmacokinetics from preclinical information: comparative accuracy of quantitative prediction approaches. *J Clin Pharmacol* **49**:513–533.

Hsyu PH, Mould DR, Abbas R, and Amantea M (2014) Population pharmacokinetic and pharmacodynamic analysis of bosutinib. *Drug Metab Pharmacokinet* **29**:441–448.

Hsyu PH, Pignataro DS, and Matschke K (2017) Effect of aprepitant, a moderate CYP3A4 inhibitor, on bosutinib exposure in healthy subjects. *Eur J Clin Pharmacol* **73**:49–56.

Huang SM, Abernethy DR, Wang Y, Zhao P, and Zineh I (2013) The utility of modeling and simulation in drug development and regulatory review. *J Pharm Sci* **102**:2912–2923.

Huang SM and Rowland M (2012) The role of physiologically based pharmacokinetic modeling in regulatory review. *Clin Pharmacol Ther* **91**:542–549.

Jamei M, Marciniak S, Feng K, Barnett A, Tucker G, and Rostami-Hodjegan A (2009) The Simcyp population-based ADME simulator. *Expert Opin Drug Metab Toxicol* **5**:211–223.

Johnson TN, Boussery K, Rowland-Yeo K, Tucker GT, and Rostami-Hodjegan A (2010) A semi-mechanistic model to predict the effects of liver cirrhosis on drug clearance. *Clin Pharmacokinet* **49**:189–206.

Jones H and Rowland-Yeo K (2013) Basic concepts in physiologically based pharmacokinetic modeling in drug discovery and development. *CPT Pharmacometrics Syst Pharmacol* **2**:e63.

Jones HM, Chen Y, Gibson C, Heimbach T, Parrott N, Peters SA, Snoeys J, Upreti VV, Zheng M, and Hall SD (2015) Physiologically based pharmacokinetic modeling in drug discovery and development: a pharmaceutical industry perspective. *Clin Pharmacol Ther* **97**:247–262.

Lavé T, Parrott N, Grimm HP, Fleury A, and Reddy M (2007) Challenges and opportunities with modelling and simulation in drug discovery and drug development. *Xenobiotica* **37**:1295–1310.

Nestorov I (2007) Whole-body physiologically based pharmacokinetic models. *Expert Opin Drug Metab Toxicol* **3**:235–249.

Pfizer (2016) Prescribing information for Bosulif (bosutinib) tablets, for oral use. Pfizer, New York.

Prueksaritanont T, Chu X, Gibson C, Cui D, Yee KL, Ballard J, Cabalu T, and Hochman J (2013) Drug-drug interaction studies: regulatory guidance and an industry perspective. *AAPS J* **15**: 629–645.

Pugh RN, Murray-Lyon IM, Dawson JL, Pietroni MC, and Williams R (1973) Transection of the oesophagus for bleeding oesophageal varices. *Br J Surg* **60**:646–649.

Rodgers T, Leahy D, and Rowland M (2005) Physiologically based pharmacokinetic modeling 1: predicting the tissue distribution of moderate-to-strong bases. *J Pharm Sci* **94**:1259–1276.

Rowland M, Peck C, and Tucker G (2011) Physiologically-based pharmacokinetics in drug development and regulatory science. *Annu Rev Pharmacol Toxicol* **51**:45–73.

Rowland Yeo K, Aarabi M, Jamei M, and Rostami-Hodjegan A (2011) Modeling and predicting drug pharmacokinetics in patients with renal impairment. *Expert Rev Clin Pharmacol* **4**:261–274.

Simcyp (2013) *A Guide for IVIVE and PBPK/PD Modeling Using the Simcyp Population-Based Simulator (Simcyp Manual Version 13)*, Simcyp Limited/Certara, Sheffield, UK.

Sinha V, Zhao P, Huang SM, and Zineh I (2014) Physiologically based pharmacokinetic modeling: from regulatory science to regulatory policy. *Clin Pharmacol Ther* **95**:478–480.

Sun H, Frassetto L, and Benet LZ (2006) Effects of renal failure on drug transport and metabolism. *Pharmacol Ther* **109**:1–11.

Syed YY, McCormack PL, and Plosker GL (2014) Bosutinib: a review of its use in patients with Philadelphia chromosome-positive chronic myelogenous leukemia. *BioDrugs* **28**:107–120.

Verbeeck RK (2008) Pharmacokinetics and dosage adjustment in patients with hepatic dysfunction. *Eur J Clin Pharmacol* **64**:1147–1161.

Vinik HR, Reves JG, Greenblatt DJ, Abernethy DR, and Smith LR (1983) The pharmacokinetics of midazolam in chronic renal failure patients. *Anesthesiology* **59**:390–394.

Wagner C, Pan Y, Hsu V, Grillo JA, Zhang L, Reynolds KS, Sinha V, and Zhao P (2015) Predicting the effect of cytochrome P450 inhibitors on substrate drugs: analysis of physiologically based pharmacokinetic modeling submissions to the US Food and Drug Administration. *Clin Pharmacokinet* **54**:117–127.

Yang J, Jamei M, Yeo KR, Tucker GT, and Rostami-Hodjegan A (2007) Prediction of intestinal first-pass drug metabolism. *Curr Drug Metab* **8**:676–684.

Zhang L, Xu N, Xiao S, Arya V, Zhao P, Lesko LJ, and Huang SM (2012) Regulatory perspectives on designing pharmacokinetic studies and optimizing labeling recommendations for patients with chronic kidney disease. *J Clin Pharmacol* **52** (Suppl):79S–90S.

Zhang Y, Zhang L, Abraham S, Apparaju S, Wu TC, Strong JM, Xiao S, Atkinson AJ, Jr, Thummel KE, Leeder JS, et al. (2009) Assessment of the impact of renal impairment on systemic exposure of new molecular entities: evaluation of recent new drug applications. *Clin Pharmacol Ther* **85**:305–311.

Zhao P, Ragueneau-Majlessi I, Zhang L, Strong JM, Reynolds KS, Levy RH, Thummel KE, and Huang SM (2009) Quantitative evaluation of pharmacokinetic inhibition of CYP3A substrates by ketoconazole: a simulation study. *J Clin Pharmacol* **49**:351–359.

Zhao P, Rowland M, and Huang SM (2012) Best practice in the use of physiologically based pharmacokinetic modeling and simulation to address clinical pharmacology regulatory questions. *Clin Pharmacol Ther* **92**:17–20.

Zhao P, Zhang L, Grillo JA, Liu Q, Bullock JM, Moon YJ, Song P, Brar SS, Madabushi R, Wu TC, et al. (2011) Applications of physiologically based pharmacokinetic (PBPK) modeling and simulation during regulatory review. *Clin Pharmacol Ther* **89**:259–267.

Address correspondence to: Dr. Shinji Yamazaki, Pharmacokinetics, Dynamics, and Metabolism, La Jolla Laboratories, Pfizer Worldwide Research and Development, 10777 Science Center Drive, San Diego, CA 92121. E-mail: shinji.yamazaki@pfizer.com